Biophysical Journal, Volume 99

Supporting Material

Characterization of Brightness and Stoichiometry of Bright Particles by Flow - Fluorescence Fluctuation Spectroscopy

Jolene L Johnson, Yan Chen, and Joachim D Mueller

Supplemental Information for "Characterization of Brightness and Stoichiometry of Bright Particles by Flow - Fluorescence Fluctuation Spectroscopy"

Jolene Johnson, Yan Chen, and Joachim D. Mueller

School of Physics and Astronomy, University of Minnesota, Minneapolis, MN 55455

Correspondence should be sent to Joachim Mueller: mueller@physics.umn.edu

Material and Methods

Sample preparation

Internally labeled green fluorescent spheres (Duke Scientific, Fremont, CA) were suspended in a buffer of 0.5% sodium dodecyl sulfate (SDS) and 14.7% sucrose. The sucrose was included to match the density of the spheres in order to avoid sedimentation. The resulting viscosity was 1.54 cP at 20^{o} Celsius. SDS was included to prevent aggregation and adsorption to surfaces. Sphere solutions were vortexed briefly, then sonicated in a water bath for 5 min immediately prior to performing experiments.

VLPs were obtained from Cos-1 cells (ATCC, Manassas, VA) transfected with Gag^{YFP} vector (1) maintained in 10% fetal bovine serum and DMEM (without phenol red). Transfection was carried out using TransFectin according to the manufacturer's protocol (BioRad, Hercules, CA). Cells were maintained at 80% confluency on the day of transfection. For a standard VLP experiment, 2.1 μg of vector and 1.25 μg of TransFectin were mixed and added to a cell culture plate with a growth area of 25 cm^2. 32 hours after transfection the cell medium was collected and spun at 14000 rpm for 2 min to eliminate cell debris. A portion of non-concentrated VLP in cell supernatant was saved for future studies. The remaining solution was concentrated by a factor of 10 into Dulbecco's PBS (Biowhittaker, Walkersville, MD) using a Centricon filter (Millipore, Billerica, MA) at 14000 rpm. The viscosity of the solution is ~1 cP at 20^{o} Celsius.

Device Fabrication

Microfluidic devices were fabricated from a master mold created by photolithography (2). The channels were made using molds fabricated with SU8 2015 photoresist (MicroChem Corp, Newton, MA). SU-8 was spincoated on a four inch silicon wafer to a thickness of 20 μm. 1:10 curer to PDMS proportioned Sylgard 184 (Dow Corning, Midland, MI) was poured over the molds to a thickness of approximately 2 mm. After curing, the PDMS was pulled off and irreversibly bonded to a #1.5 coverslip glass using a plasma oxygen oven with a 30 sec exposure at 0.2 Torr. The seal was solidified by heating on a hot plate for 1 hour at 75^{o}C. Holes were punched from the top of the elastomer block at either end of the channel into which tubing was inserted. Prior to use each channel was rinsed and soaked with buffer overnight to avoid solvent permeation effects.

Calibrations

A study of the fluorescence intensity was performed as a function of the excitation power for the microsphere and VLP samples to determine the excitation power range that avoids unwanted optical effects such as photobleaching and saturation (3, 4). The beam waist was calibrated from an FCS measurement of 26 nm diameter, internally labeled fluorescent spheres (Duke Scientific, Fremont, CA) in aqueous solution. The diffusion coefficient calculated from the Stokes-Einstein relation was used to convert the diffusion time into a beam waist of 0.38 ± 0.02 μm. The optical observation volume V_O was calibrated by PCH analysis of a dye solution with known concentration c = 80 nM using $V_O = N/(c \cdot N_A)$, where N_A is Avogadro's number. The calibration returned a sample volume of 0.08 – 0.15 fL depending on instrument parameters and the index of refraction of the measured sample. All channel measurements were performed at the

center of the channel unless otherwise noted because this area has the smallest velocity gradient as a function of height.

Occasionally, an unusually high intensity spike with an amplitude 3-10 times that of any other peaks was observed during an FFS experiment. The spike most likely represents the passage of a large fluorescent aggregate. Data sets with a spike were typically retaken. If retaking the data was impractical, the spike was removed by software from the raw data before analysis.

Theory

The next sections describe the influence of flow on the probability distribution function of the fluorescence intensity and the photon counts.

The probability distribution function of fluorescence for diffusion and flow

An FFS experiment detects the fluorescence $F(t)$ of particles present within a small optical observation volume. The observation volume $O(\mathbf{r})$ is typically approximated by a 3 dimensional Gaussian (3DG) or by a squared Gaussian-Lorentzian (GL) function, which for convenience is normalized to one at the origin, $O(0)=1$. The observation volume is defined by $V_O = \int O(\mathbf{r}) d\Omega$. The instantaneous fluorescence $F(t)$ is time-dependent, because the particles are free to move, which gives rise to fluctuations in the signal as they pass through the observation volume. Statistical analysis of FFS data requires that the process which gives rise to the fluctuations is stationary. By definition, a stationary process is a stochastic process whose probability distribution function (pdf) does not change when shifted in time or space. In other words, in order to apply FFS, the pdf $p(F)$ of the fluorescence has to be a constant function with respect to time and space. In addition, the autocorrelation function of a stationary process only depends on the time difference τ, but not on the absolute time.

Diffusion is a stationary process with a time and space independent probability distribution function, $p_{\#}(n)$, of finding *n* particles at a small volume element located at **r**. The pdf $p(F)$ of the fluorescence is $p(F) = \int_{\Omega} \delta\left(F - \lambda \cdot O(\mathbf{r})\right) \cdot p_{\#}(n) d\Omega$, where λ is the brightness of a single particle in units of counts per second (cps), δ is Dirac's-delta function, and integration is carried out over the sample volume Ω. Note that flow corresponds to a translation of the sample in space. Because $p_{\#}(n)$ is independent of time and space, a translation in space does not affect the functional form of $p_{\#}(n)$. Consequently, the presence or absence of flow does not affect the pdf $p(F)$ of the fluorescence. Because $p(F)$ uniquely determines the moments of *F*, the variance and mean of the fluorescence are identical whether flow is present or not. Hence, the fluctuation amplitude $g(0) \equiv \langle \Delta F^2 \rangle / \langle F \rangle^2$ and Mandel's Q-parameter $Q \equiv \langle \Delta F^2 \rangle / \langle F \rangle$ are independent of flow.

Sampling time and flow

We previously pointed out that $p(F)$ is independent of the presence of flow. However, the detector records the fluorescence integrated over a finite sampling time T (5),

$$W(t) = \int_{t-T/2}^{t+T/2} F(t')\,dt' . \tag{S1}$$

If the sampling time T is faster than the time scale of fluorescence intensity fluctuations, then the integrated intensity W faithfully tracks the intensity F and Eq. S1 is approximated by

$$W(t) = F(t)T . \tag{S2}$$

In this manuscript we choose experimental conditions where this approximation is valid. Because the experiment tracks the instantaneous fluorescence $F(t) = W(t)/T$, the conclusion that the probability distribution and moments of F or W are independent of flow remains valid (6).

However, the rate of intensity fluctuations increases with the flow speed. Once the flow speed is sufficiently high, the approximation (Eq. S2) breaks down. We refer to these conditions, where the sampling time T is insufficient to track $F(t)$, as undersampling. Under these circumstances, rapid fluctuations are integrated out and the statistical properties, such as the pdf and the moments of W, now explicitly depend on the flow speed. Thus, the flow speed v_F has to be kept below a critical value, which depends on the sampling time T and beam waist, in order to ensure the validity of Eq. S2. We determine the critical flow speed by observing the onset of flow speed dependent changes in the pdf or moments of W.

Photon Counting Histogram (PCH)

Until now we ignored the fact that a photon counting detector records the number of photon counts k in the sampling time T instead of the integrated intensity W. Mandel's formula relates the pdf $p(W)$ of the integrated light intensity W absorbed by the detector to the pdf $p(k)$ of the photon counts k (7). We refer to $p(k)$ as the photon counting histogram. In the absence of undersampling Mandel's formula determines PCH by (6)

$$p(k) = \int_0^\infty \mathrm{Poi}(k, F \cdot T)\, p(F)\, dF , \tag{S3}$$

where $\mathrm{Poi}(k,x)$ is the Poisson distribution with an average photon count of x. Because $p(F)$ is independent of flow speed, the PCH $p(k)$ is also independent of flow speed as long as undersampling is avoided. Because the PCH determines the brightness λ and concentration N of each fluorescent species in the sample, these parameters are independent of flow speed in the absence of undersampling.

Supplementary Figure S1

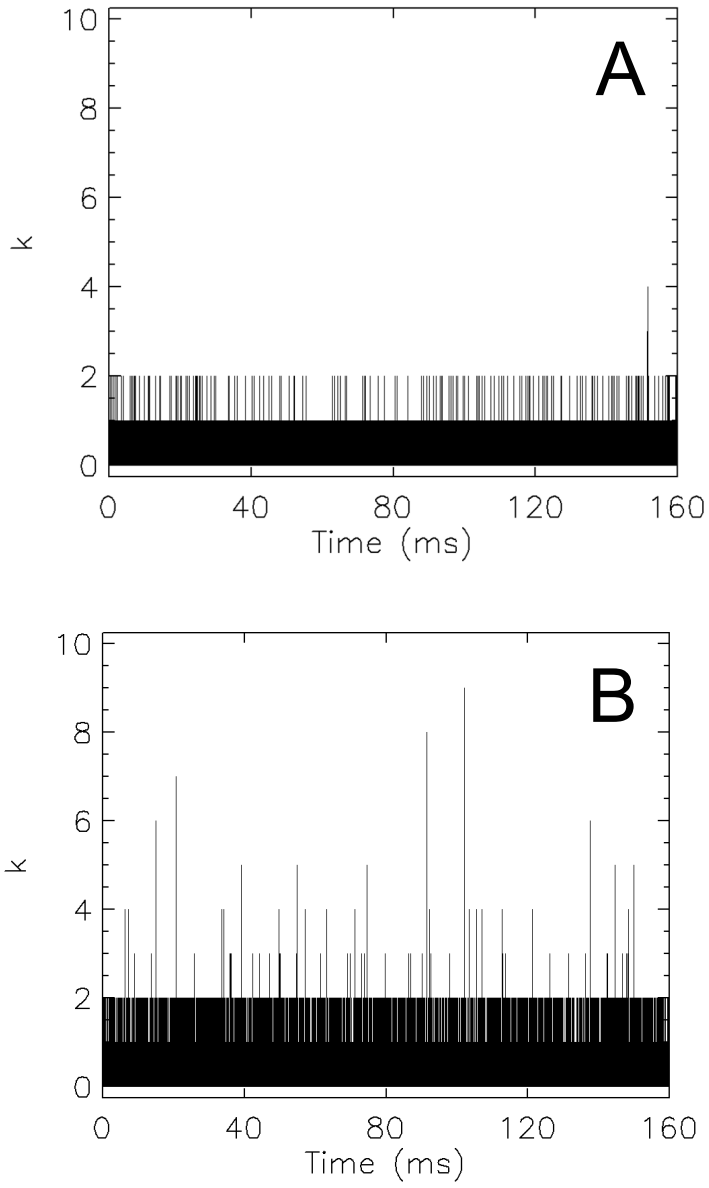

Fig S1. Intensity traces of a low concentration sample with and without flow. 100 nm fluorescent spheres at a concentration of 110 fM were measured with and without flow for 160 s at a sampling frequency of 200 kHz. (A). The intensity trace of a stationary sample showing a single event. (B). The intensity trace of the same sample flowing at 8.7 mm/s. Flow provides a sufficient increase in the event rate to make FFS analysis feasible.

Supplementary Figure S2

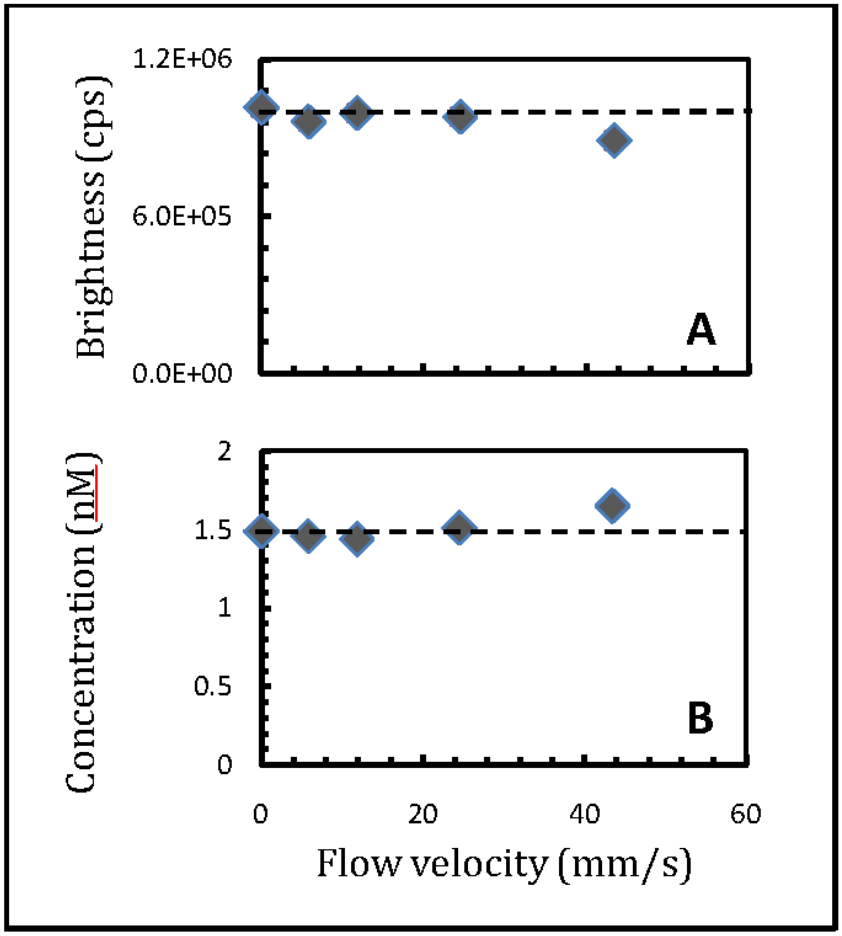

Fig S2. Brightness and concentration versus flow velocity. The velocity of a sample with 100-nm diameter fluorescent spheres at 1.5 nM was varied from 0 to 44 mm/s. Both the brightness (A) and concentration (B) determined by PCH analysis are independent of flow speed in the range from 0 to 25 mm/s. Undersampling is observed at a speed of 44 mm/s, which leads to an apparent increase in the particle concentration and a decrease in the brightness. The error was determined from the standard deviation of multiple measurements (n = 4) at each velocity. The symbol size is larger than the error.

References

1. Derdowski, A., L. Ding, and P. Spearman. 2004. A novel fluorescence resonance energy transfer assay demonstrates that the human immunodeficiency virus type 1 Pr55Gag I domain mediates Gag-Gag interactions. J Virol 78:1230-1242.
2. Duffy, D. C., J. C. McDonald, O. J. A. Schueller, and G. M. Whitesides. 1998. Rapid Prototyping of Microfluidic Systems in Poly(dimethylsiloxane). Analytical Chemistry 70:4974-4984.
3. Berland, K., and G. Shen. 2003. Excitation saturation in two-photon fluorescence correlation spectroscopy. Applied optics 42:5566-5576.
4. Patterson, G. H., and D. W. Piston. 2000. Photobleaching in two-photon excitation microscopy. Biophysical journal 78:2159-2162.
5. Müller, J. D. 2004. Cumulant analysis in fluorescence fluctuation spectroscopy. Biophys. J. 86:3981-3992.
6. Chen, Y., J. D. Müller, P. T. C. So, and E. Gratton. 1999. The photon counting histogram in fluorescence fluctuation spectroscopy. Biophys. J. 77:553-567.
7. Mandel, L. 1958. Fluctuations of photon beams and their correlations. Proc. Phys. Soc. 72:1037-1048.